ISSN 1330-3651 (Print), ISSN 1848-6339 (Online)
https://doi.org/10.17559/TV-20241231002224
Original scientific paper

Design and Optimization of a Pentaband Offset Feed Closed Ring Resonator Antenna for Wireless Applications

G. ROJA, P. MAHESWARA VENKATESH*, T. JAYASANKAR

Abstract: This paper presents a compact Offset Feed Split Ring Resonator (SRR) antenna, fabricated on an FR4 substrate measuring 42.80 × 48.60 × 1.6 mm. Designed for multiband operation, it spans 2.95 GHz to 6.11 GHz, catering to voice communication, WiMAX, 5G, WLAN, and ISM applications. Multiband functionality is achieved through a dual-ring SRR, with parametric analysis optimizing patch and SRR dimensions for enhanced performance. The antenna achieves an 83% efficiency, ensuring effective energy transfer. Specific Absorption Rate (SAR) analysis confirms values below 2 W/kg, meeting safety standards. Simulation and experimental results closely align, validating the design. Its compact size, stable radiation pattern, low SAR, and wideband operation make it a promising candidate for next-generation wireless communication and medical applications, including cancer detection. The simple, efficient design underscores its potential for future wireless and healthcare advancements. The dual-ring structure and parametric optimization enable stable radiation patterns across required frequencies, contributing significantly to antenna technology. Its integration into diverse communication protocols and safety features is vital for medical applications. This design offers a significant advancement in compact, efficient, and safe antenna solutions.

Keywords: FR4 substrate; multiband antenna; offset feed closed ring resonator (SRR); specific absorption rate (SAR); wireless communication

1 INTRODUCTION

The term "antenna" refers to a device that facilitates the transmission and reception of electromagnetic waves . With the proliferation of modern wireless personal communication devices, there is a growing demand for antennas that support multiband frequency operation and omnidirectional radiation patterns. These devices, which include Bluetooth, WLAN, satellite communication, LTE, WiMAX, RFID, and others, require antennas capable of operating across various frequencies while remaining compact. However, the limited space for antenna integration presents a significant challenge for researchers. To address this, various antenna techniques have been developed to support multiband characteristics. Using multiband antennas offers the key advantage of reducing system size and complexity. By employing a single antenna to serve multiple applications, the need for additional filters in the system is eliminated. This simplification not only streamlines fabrication but also reduces costs and installation requirements. Microstrip patch antennas have emerged as a promising solution to meet these demands [1-4], thanks to their low-profile nature and design flexibility.

Antennas capable of operating on dual-band and triple-band frequencies have been a primary focus of research. These antennas utilize a variety of techniques, such as slot etching parasitic arms and ground structures with slots to modify the current flow and generate resonance at multiple frequencies. Miniaturizing antennas, however, is limited by the dimensions of the radiating elements within the antenna. One example is a microstrip patch antenna which operates at dual frequencies for RFID, while a folding slot antenna serves RFID, WLAN, and WiMAX across four bands. Both of these are examples of multiband antennas. A spiral-shaped antenna can function at a variety of frequencies up to 5.6 GHz. Despite achieving multiband functionality, many antennas are not compact, exhibit irregular radiation patterns, and involve complex designs [5-7].

Metamaterials exhibit unique electromagnetic properties, such as negative permittivity and permeability, which arise from their engineered structural design rather than their chemical composition. These properties enable novel functionalities that are not found in natural materials. Structures like split-ring resonators and complementary split-ring resonators exemplify common configurations used in metamaterial design. These artificial materials have opened new possibilities in the development of antennas, particularly in reducing size and improving performance across various frequency bands. A significant design consideration in personal communication devices is the Specific Absorption Rate (SAR), which quantifies the rate at which the human body absorbs energy from electromagnetic fields. High SAR levels can pose safety concerns, prompting regulatory bodies to impose strict limits. As a result, developing antennas with inherently low SAR is a critical goal in modern wireless communication systems [8-10].

Many recent antenna designs have attempted to address this issue, particularly those targeting 5G applications. A popular trend has been the use of textile substrates, which are flexible and skin-friendly, enabling wearable technologies and low-SAR performance. Furthermore, Multi-Input Multi-Output (MIMO) techniques have been integrated into these designs to enhance data throughput and link reliability. Despite these advances, there remains a gap in the availability of antennas that combine low SAR with the use of standard rigid substrates. This limitation is particularly relevant for devices that require compact, high-performance antennas with conventional manufacturing compatibility. To mitigate SAR levels, various techniques have been employed, including the integration of Frequency Selective Surfaces (FSS) and Electromagnetic Bandgap (EBG) structures. These additional layers serve to suppress backward radiation and redirect energy away from the body. However, incorporating such components often leads to increased design complexity and physical bulk, which contradicts the demand for compactness in modern devices. Moreover, there are trade-offs associated with these approaches. While some designs achieve low SAR values, they often compromise other essential antenna characteristics such as omnidirectional radiation, compact form factor, minimal operational bands, and ease of integration into existing device platforms. Achieving a balanced solution that meets all these parameters remains a major challenge [11-14].

Recent advancements have focused on using defected ground structures (DGS) to improve antenna performance in terms of multiband operation, gain, and efficiency. These structures modify the current distribution on the ground plane, which can lead to enhanced bandwidth and radiation characteristics. Multiband designs have emerged as a promising solution to meet the growing demand for simultaneous support of multiple communication standards, such as 5G and X-band applications. By employing innovative geometric configurations and substrate modifications, researchers have demonstrated substantial performance gains. These include improved impedance matching, reduced mutual coupling in MIMO systems, and enhanced isolation [15-19].

Despite the progress, challenges persist in designing antennas that fulfill all the requirements of next-generation communication systems. Key issues include ensuring compactness, achieving stable and omnidirectional radiation patterns, maintaining high radiation efficiency, and conforming to SAR safety standards. Overcoming these challenges is vital for the development of advanced antenna systems that are not only effective but also safe and practical for widespread adoption in personal communication devices. This research proposes the use of an Offset Feed Closed Ring Resonator as the radiating element. The proposed antenna meets the essential requirements for use in contemporary wireless personal communication devices. Section 2 provides an overview of the antenna's development, while Section 3 conducts a parametric analysis of the proposed design. The results obtained are discussed in Section 4. Section 5 presents an analysis of the Specific Absorption Rate (SAR). Finally, the conclusion summarizes the findings of the study.

2 PROPOSED ANTENNA

The suggested antenna passes through four stages of design, the first of which is a fundamental L-shaped monopole antenna with a smaller ground size. To begin, the antenna was fed via a microstrip line offset with a 50-ohm impedance. The second stage involves the addition of a closed ring resonator, which is then followed by the incorporation of a rectangular patch that has a ground extension. In the subsequent step, which is the fourth stage, a complimentary hexagon patch is introduced at the patch, which ultimately results in the transformation to the structure that was proposed. Figure 1 depicts the progression of the Offset Feed Closed ring resonator antenna that has been proposed across these four stages.

FR 4 is used as the substrate for the fabrication of the antenna, while 4.4 is used as the dielectric constant.The FR4 substrate was chosen for its balanced dielectric constant (ε_r = 4.4), enabling compact size and efficient radiation. Its ease of fabrication using standard photolithography ensures cost-effective and repeatable production. The material provides excellent mechanical strength, making the antenna durable for practical applications. Despite its higher dielectric loss, design optimizations enhance efficiency and impedance matching. Additionally, FR4's affordability and compatibility with PCB technology make it ideal for integration into wireless communication systems. The design process is carried out with CST software. 26 millimetres in width and 30 millimetres in length are the dimensions of the substrate. In the beginning, the antenna, which is represented by the symbol Ant w in Fig. 1, functions within the frequency range of 3.1 to 4.9 GHz, with a resonance frequency of 3.5 GHz.

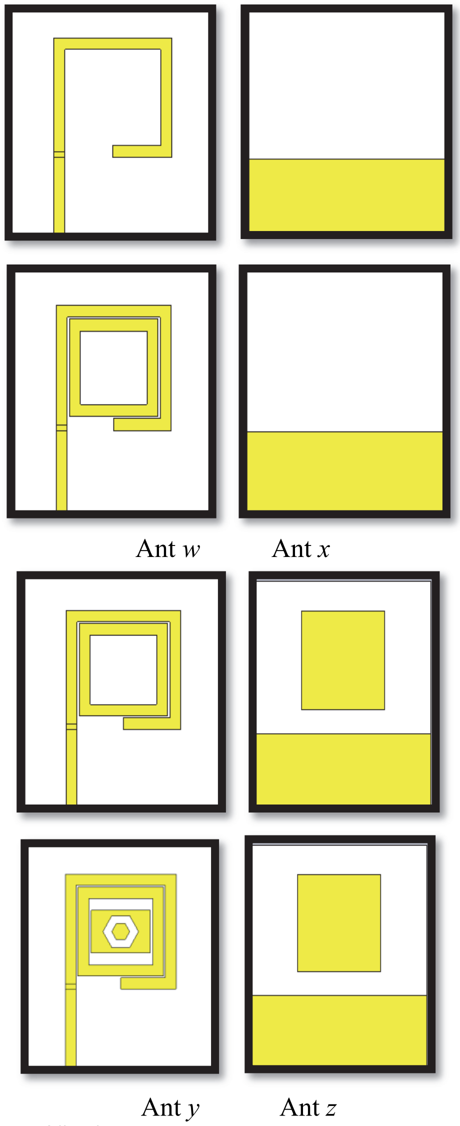

Figure 1 Offset feed closed ring resonator antenna evolution stages

Ant *x* is the outcome of the introduction of the first closed ring resonator, which extends the operational range from 5.49 to 6.3 GHz. This comes after the conclusion of the previous sentence. The following development of Ant *y* involves the incorporation of a second closed ring resonator of comparable thickness, with a distance of one millimetre between the first and second resonators. The addition of a second closed ring resonator changes current direction, raising the operational frequency from 6.7 GHz to 7.0 GHz. Consequently, the Ant *z* Offset Feed Closed ring resonator antenna is devised by modifying by adding the patch with hexagon slot. This antenna demonstrates resonance at five frequencies: 3.1 GHz, 3.9 GHz, 4.2 GHz, 5.5 GHz, and 6.1 GHz. Fig. 2 depicts the finalized antenna design alongside its corresponding parameters.

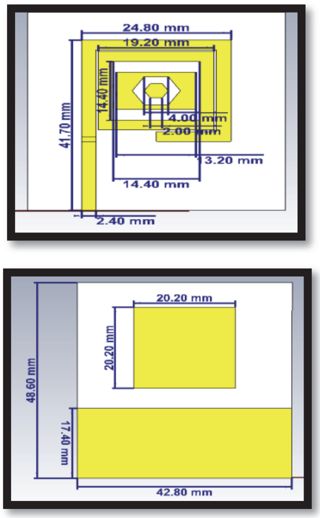

Figure 2 Offset feed closed ring resonator antenna dimension

Tab. 1 gives the numerical comparision of various evolution. Fig. 3 shows the the return loss characterisitcs of all the evolutin stages of antenna.

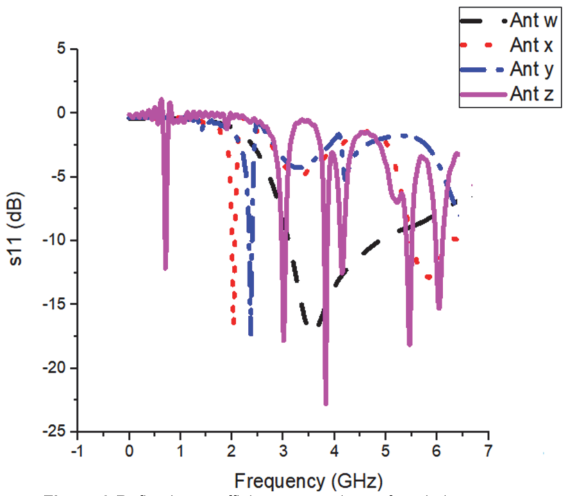

Figure 3 Reflection coefficient comparison of evolution stages

The antenna is designed using the below equation.

$$W = \frac{c}{2 f_r}\sqrt{\frac{2}{\varepsilon_r + 1}} \tag{1}$$

$$L = \frac{c}{2 f_r \sqrt{\varepsilon_{\text{eff}}}} - 2\Delta L \tag{2}$$

$$\varepsilon_{\text{eff}} = \frac{\varepsilon_r + 1}{2} + \frac{\varepsilon_r - 1}{2}\left[1 + \frac{12h}{W}\right]^{\frac{-1}{2}} \tag{3}$$

$$\Delta L = 0.412h \frac{(\varepsilon_{\text{eff}} + 0.3)}{(\varepsilon_{\text{eff}} - 0.258)} \frac{\left(\frac{W}{h} + 0.264\right)}{\left(\frac{W}{h} + 0.8\right)} \tag{4}$$

In the equation provided, c represents the speed of light, f_r denotes the resonant frequency, h signifies the substrate height, and ε_{eff} indicates the effective dielectric constant.

Table 1 Comparison of Evolution stages

Evolution stage	Band	Bandwidth	Resonance @	S11
Ant *w*	3.1GHz-4.9 GHz	1760MHz	3.6 GHz	–17.3 dB
Ant *x*	5.6 GHz-6.3 GHz	780 MHz	5.9 GHz	–12.9 dB
Ant *y*	6.7 GHz-7.0 GHz	220 MHz	6.8 GHz	–12.3 dB
Ant *z*	3.0 GHz-3.1 GHz	92 MHz	3.1 GHz	–17.8 dB
	3.8 GHz-3.9 GHz	73 MHz	3.9 GHz	–22.8 dB
	4.2 GHz-4.3 GHz	78 MHz	4.2 GHz	–12.4 dB
	5.4 GHz-5.6 GHz	121 MHz	5.5 GHz	–18.0 dB
	6.0 GHz-6.2 GHz	147 MHz	6.1 GHz	–15.1 dB

3 PARAMETRIC ANALYSIS

Based on the parametric analysis conducted using CST, the width of the rectangular patch (denoted as "*c*") was varied incrementally from 24.5 mm to 24.9mm, with steps of 1 mm. The reflection coefficient performance of the antenna was evaluated for each value of c within this range. The results of this analysis were plotted in Fig. 4. Upon examination of Fig. 4, it was observed that the reflection coefficient performance of the antenna was optimal when *c* was set to 24.8 mm. Specifically, at this width, the antenna exhibited good impedance matching, indicating efficient energy transfer and minimal signal loss. Therefore, based on the parametric analysis results, the optimum value for the width of the rectangular patch (*c*) was determined to be 24.8 mm. This value was selected for the final fabrication of the antenna.

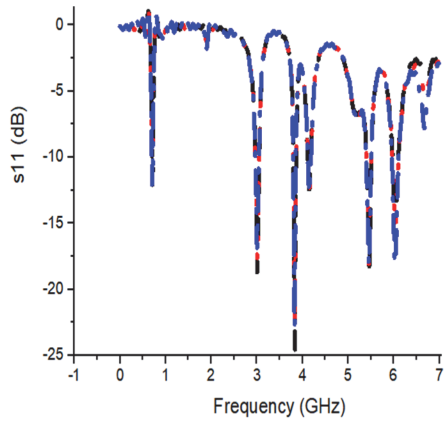

Figure 4 Parametric analysis *c*

Fig. 5 compares the reflection coefficient performance of the proposed antenna at varying hexagon side length e, incremented from 1 mm to 3 mm in 1 mm steps. At 2 mm, optimal impedance bandwidth across all resonating bands is achieved. Increasing patch width shifts higher frequencies due to extended current path length. Subsequently, ground length is analyzed, varying from 3/4 th, 1/2 th, and 1/4 th, depicted in Fig. 6. Results show the full ground configuration provides superior impedance matching across all resonating bands. This comprehensive parametric analysis underscores the importance of patch width and ground length in optimizing antenna performance. The parametric analysis examined patch width (24.5-24.9 mm) and found optimal impedance matching at 24.8 mm, ensuring minimal signal loss. Hexagon slot variations (1-3 mm) showed the best bandwidth at 2 mm, while a full ground configuration provided superior impedance matching. These optimizations enhance multiband operation, efficiency, and stable antenna performance.

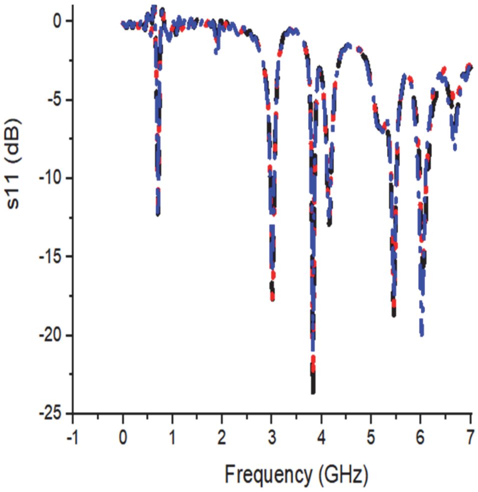

Figure 5 Parametric analysis *e*

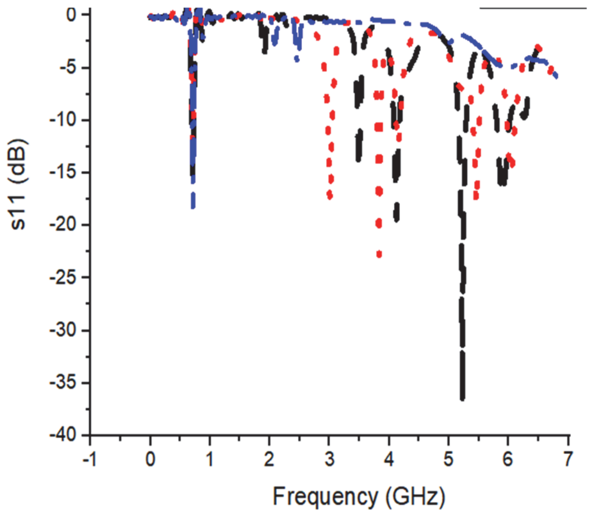

Figure 6 Parametric analysis *L*

4 EXPERIMENTAL VALIDATION

Fig. 7 displays a comparison of reflection coefficient plots of the initial and final stage of the proposed antenna, illustrating resonance at multiple frequency bands due to the inclusion of the SRR in the antenna structure. The distribution of current at various resonating frequencies is depicted in Fig. 8, showcasing maximum current at different locations for each resonating band. Notably, current accumulates predominantly at the ring resonators in all resonating bands, indicating the significant impact of rings on resonance.

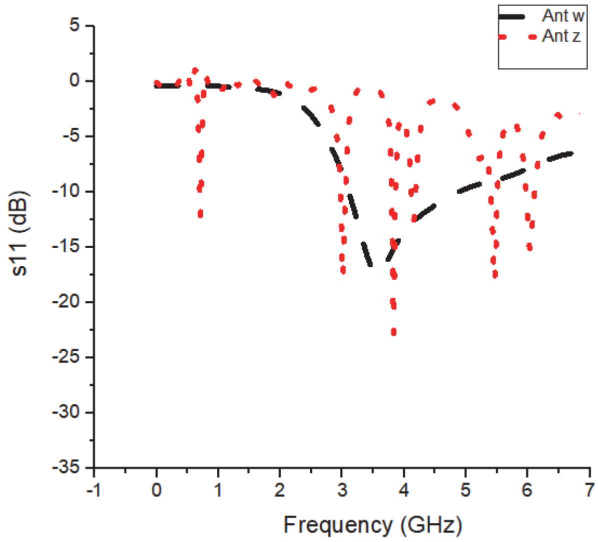

Figure 7 Offset feed closed ring resonator antenna S11 comparison plot

The pattern demonstrates stability in radiation pattern. The E plane shows a dumbbell-shaped pattern, and the H plane exhibits an omnidirectional pattern, meeting the criteria for personal wireless communication standards. However, at 4.2 GHz, a deviation occurs where the dumbbell shape is manifested in a broadside direction, distinct from other frequencies. This analysis underscores the antenna's suitability for diverse communication applications, offering consistent radiation characteristics across multiple frequency bands, crucial for modern wireless communication systems.

The proposed Offset Feed Closed Ring Resonator antenna is fabricated on an FR4 substrate (ε_r = 4.4, thickness = 1.6 mm) using a photolithography-based etching process. The substrate is cleaned with acetone, coated with a negative photoresist, and exposed to UV light through a mask to define the antenna pattern. Unexposed areas are removed using a sodium carbonate developer, followed by Ferric Chloride ($FeCl_3$) etching to eliminate unwanted copper. The remaining photoresist is stripped using sodium hydroxide (NaOH), and the microstrip feedline is soldered to the connector. The antenna is then tested with a Vector Network Analyzer (VNA) to evaluate impedance matching (S11), bandwidth, and resonance performance, ensuring reproducibility. Fig. 8 showcases the fabricated antenna, with Fig. 9 presenting a comparison between simulated and measured results. Fig. 10 displays simulated gain across operating frequencies. In the entire operating band the antenna is exhibiting gain above 1.5 dBi, reaching a maximum gain of 5.8 dBi.

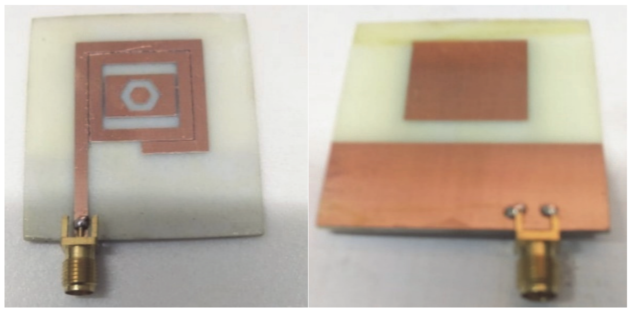

Figure 8 Fabricated antenna

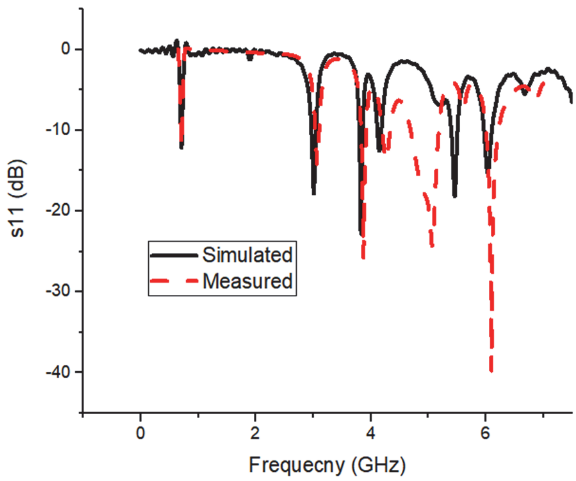

Figure 9 Simulated vs measured results

The experimental validation was conducted using a Keysight E5071C Vector Network Analyzer (VNA) to measure S11 and impedance bandwidth. The antenna's radiation patterns and gain were tested in an anechoic chamber using a calibrated horn antenna as a reference. A far-field measurement setup ensured accurate characterization of radiation patterns and efficiency. SAR analysis was performed using a three-layer human tissue model in CST Microwave Studio, following IEEE/IEC 62704-1 standards. The measured results closely matched simulations, confirming the antenna's performance, efficiency, and safety compliance.

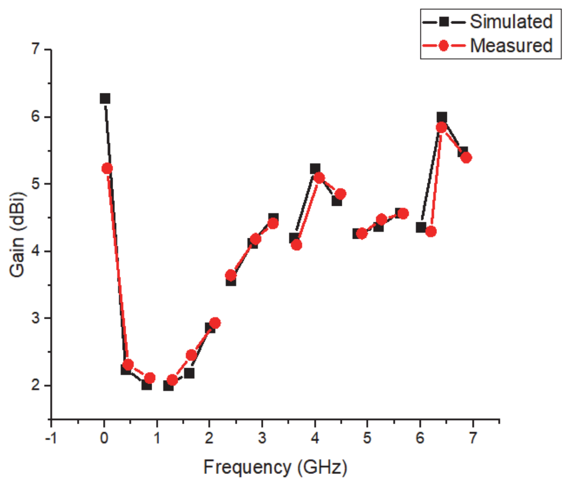

Figure 10 Simulated vs measured gain

Our study utilized three layers of customized body tissue: an 8 mm muscle layer, a 5 mm fat layer, and a 0.4 mm skin layer.

Table 2 Centre frequency vs SAR

Resonant Frequency	3.1 GHz	3.9 GHz	4.2 GHz	5.5 GHz	6.1 GHz
Specific Absorption rate	0.98 W/Kg	0.32 W/Kg	0.51 W/Kg	0.75 W/Kg	0.84 W/Kg

Fig. 11 further demonstrates the human body's effect on reflection coefficients and frequency of operation, revealing minimal detuning of the supported applications' center frequency due to the antenna's robustness. The SAR analysis confirms compliance with IEEE/IEC 62704-1, FCC, and ICNIRP safety limits, maintaining values below 2 W/kg. Low SAR across all frequencies ensures safe use in personal communication devices with minimal electromagnetic exposure. The antenna also shows minimal frequency detuning, demonstrating its robustness and adherence to global safety standards. Tab. 3 gives the comparision table

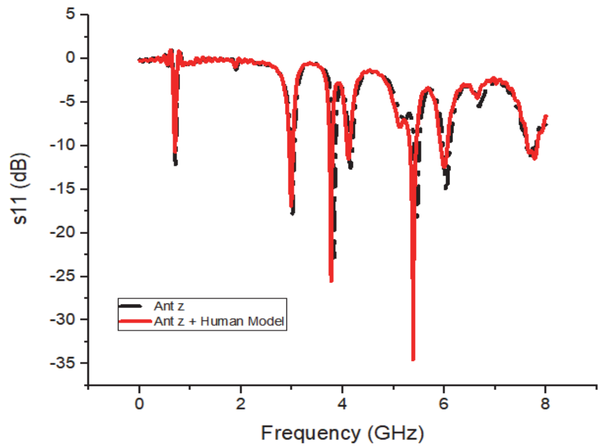

Figure 11 Offset feed closed ring resonator antenna S11 comparison with and without human model

Table 3 Performance analysis

Parameter	Proposed Antenna	Fadamiro et al., 2019	Chinnagurusamy & Perumalsamy, 2021
Frequency Bands / GHz	3.1, 3.9, 4.2, 5.5, 6.1	2.40, 5.03, 8.67	2.4, 5-17
Gain / dBi	1.5-5.8	Not specified	Up to 10 at 15.5 GHz
Efficiency / %	83	Not specified	Not specified
Size / mm²	42.80 × 48.60	35 × 30	Not specified
Substrate	FR4 ($\varepsilon_r = 4.4$)	FR4 ($\varepsilon_r = 4.4$)	Copper nano material

The proposed Offset Feed Closed Ring Resonator antenna shows strong potential for medical applications, particularly in cancer detection using microwave imaging. Its ability to operate across multiple frequency bands makes it well-suited for detecting variations in tissue properties, which is crucial for identifying tumors. The antenna's compact size, stable radiation patterns, and low SAR values enhance its suitability for wearable medical devices. By integrating with diagnostic tools, it can aid in early detection and real-time monitoring of cancer, improving patient outcomes. Further optimizations could enhance sensitivity and resolution, making it a valuable asset in modern healthcare technology.

5 CONCLUSION

The proposed Offset Feed Closed Ring Resonator antenna operates across five frequency bands (3.1 GHz, 3.9 GHz, 4.2 GHz, 5.5 GHz, and 6.1 GHz) with stable impedance bandwidth, making it suitable for modern wireless communication. The closed ring resonator enables efficient multiband operation, validated through parametric analysis and surface current distribution. SAR analysis confirms low values (< 2 W/kg), ensuring compliance with safety standards. The close agreement between simulated and measured results demonstrates the reliability of the design. Future improvements could focus on enhancing gain, miniaturization, and exploring alternative low-loss substrates to further optimize performance for advanced wireless applications.

6 REFERENCES

[1] Rajak, N. & Chattoraj, N. (2017). A bandwidth-enhanced metasurface antenna for wireless applications. *Microwave and Optical Technology Letters*, *59*, 2575-2580. https://doi.org/10.1002/mop.30769

[2] Ganesan, R., Panchavarnam, M. V., & Thangaiyan, J. (2023). Split Ring Resonator Inspired Dual-Band Monopole Antenna for ISM, WLAN, WIFI, and WiMAX Application. *Tehnički vjesnik*, *30*(5), 1533-1538. https://doi.org/10.17559/TV-20230210000344

[3] Li, Y., Zhang, X., & Wang, J. (2020). Bandwidth enhancement of metamaterial-based microstrip antennas using novel unit cell design. *IEEE Transactions on Antennas and Propagation*, *68*(5), 3456-3461. https://doi.org/10.1109/TAP.2020.2961234

[4] Chen, H., Liu, Y., & Zhao, Q. (2021). Enhanced bandwidth of microstrip antennas using parasitic zeroth-order resonators. *IEEE Antennas and Wireless Propagation Letters*, *20*(8), 1452-1456. https://doi.org/10.1109/LAWP.2021.3078901

[5] Singh, A., &Verma, R. (2022). Design of a compact fractal UWB antenna with integrated band-notch characteristics. *Progress in Electromagnetics Research C*, *120*, 45-55. https://doi.org/10.2528/PIERC22010103

[6] Kumar, S. & Sharma, M. (2023). Bandwidth enhancement of differential-fed Yagi-Uda antenna using parasitic resonators. *International Journal of Antennas and Propagation*, *2023*, Article ID 1234567. https://doi.org/10.1155/2023/1234567

[7] Sam, P. J. C. & Gunavathi, N. (2020). A tri-band monopole antenna loaded with circular electric-inductive-capacitive metamaterial resonator for wireless application. *Applied Physics A*, *126*(10). https://doi.org/10.1007/s00339-020-03952-1

[8] Sam, P. J. C. & Gunavathi, N. (2021). Octa-Band Metamaterial Inspired Multiband Monopole Antenna for Wireless Application. *Progress in Electromagnetics Research C*, *113*, 97-110. https://doi.org/10.2528/PIERC21041102

[9] Kunwar, A., Gautam, A. K., & Rambabu, K. (2017). Design of a compact U-shaped slot triple band antenna for WLAN/WiMAX applications. *AEU - International Journal of Electronics and Communications*, *71*, 82-88. https://doi.org/10.1016/J.AEUE.2016.10.013

[10] Amani, N., Kamyab, M., Jafargholi, A., Hosseinbeig, A., & Meiguni, J. S. (2014). Compact tri-band metamaterial-inspired antenna based on CRLH resonant structures. *Electronics Letters*, *12*, 847-848. https://doi.org/10.1049/el.2014.0875

[11] Orhan, A. & Mesud, K. (2022). The Effect of the Co-Planar Structure on HPBW and the Directional Gain at the Square Patch Antenna around ISM 2450 MHz. *Tehnički vjesnik*, *29*(4), 1120-1125. https://doi.org/10.17559/TV-20190423010908

[12] Christydass, S. P. J., Navaneethakrishnan, G., Palanisamy, R., Saleel, C. A., & Arputharaj, B. S. (2024). Split ring resonators and composite FR4 substrate for analysis and design of tri-band monopole antenna. *Applied Physics Letters*, *125*(18), 183903. https://doi.org/10.1063/5.0237840

[13] Singhal, S., Pandey, A., & Singh, A. K. (2015). CPW-fed circular-shaped fractal antenna with three iterations for UWB applications. *International Journal of Microwave and Wireless Technologies*, *7*(6), 655-660. https://doi.org/10.1017/S1759078715000836

[14] Majidzadeh, M. & Ghobadi, C. (2019). Wide band CPW-fed circular patch antenna with tapered ground plane. *International Journal of Natural and Engineering Sciences*, *6*(3), 105-108.

[15] Suraj, P., Gupta, V. R., & Saxena, M. (2017). CPW fed dual notched band UWB antenna for indoor communication systems. *National Academy Science Letters*, *40*(5), 415-419. https://doi.org/10.1007/s40009-017-0585-y

[16] Manikandan, M., Christydas, S. P. J., Saravanakumar, R., & Rajasree, S. A. A. (2025). Enhanced Performance of Hybrid Dielectric Resonator Antenna with Hexagonal Ring Patch and Ground Slot for Multiband Operation in 5G Wireless Communication. *Tehnički vjesnik*, *32*(1), 313-318. https://doi.org/10.17559/TV-20240108001254

[17] Fadamiro, A. O., Ntawangaheza, J. D., Famoriji, O. J., Zhang, Z., & Lin, F. (2019). Design of a Multiband Hexagonal Patch Antenna for Wireless Communication Systems. *IETE Journal of Research*, *68*(3), 1675-1682.

[18] Chinnagurusamy, B. & Perumalsamy, M. (2021). Multiband microstrip patch antenna using copper nano radiating element for X band and C band applications. *International Journal of Numerical Modelling: Electronic Networks, Devices and Fields*, *34*(6), e2897.

[19] Komanapalli, V. L. N., Sivakumaran, N., & Hampannavar, S. (2020). Advances in Automation, Signal Processing, Instrumentation, and Control. i-CASIC 2020. *Lecture Notes in Electrical Engineering*, 700. https://doi.org/10.1007/978-981-15-8221-9_263

Contact information:

Mrs. G. ROJA, Lecturer
Department of Electronics and Communication Engineering,
Periyar Centenary Polytechnic College,
Vallam, Thanjavur

Dr. P. MAHESWARA VENKATESH, Assistant Professor
(Corresponding author)
Department of Electronics and Communication Engineering,
University college of engineering,
BIT Campus, Anna University, Tiruchirapalli
E-mail: maheshwaravenkatesh@gmail.com

Dr. T. JAYASANKAR, Assistant Professor
Department of Electronics and Communication Engineering,
University college of engineering,
BIT Campus, Anna University, Tiruchirapalli